

A BGK-penalization asymptotic-preserving scheme for the multispecies Boltzmann equation *

Shi Jin[†] Qin Li[‡]

Abstract

An asymptotic preserving scheme is efficient in solving multiscale problems where both kinetic and hydrodynamic regimes co-exist. In this paper we extend the BGK-penalization based asymptotic preserving scheme, originally introduced by Filbet and Jin for the single species Boltzmann equation, to its multispecies counterpart. For the multispecies Boltzmann equation the new difficulties emerge due to: 1) the breaking down of the conservation law for each species; 2) different time scalings of convergence to the equilibriums for disparate masses. We select a suitable local Maxwellian—which is based on the mean velocity and mean temperature—as the penalty function, and justifies various asymptotic properties of this method, for both the multispecies Boltzmann equation and a disparate masses system. This results an asymptotic-preserving scheme for the multispecies Boltzmann equation that can capture the fluid dynamic limit with time step and mesh size much larger than Knudsen number, yet the numerical method does not contain any nonlinear nonlocal implicit solver. Numerical examples demonstrate the correct asymptotic-behavior of the scheme.

1 Introduction

In kinetic theory, the Boltzmann equation is a fundamental equation to describe the evolution of rarefied gases. In this paper, we are interested in numerical solution of the Boltzmann equation for multispecies gas mixture. The most basic example is high altitude gas, which could be modeled as a binary mixture of Oxygen and Nitrogen. Other applications of gas mixture may come from nuclear engineering or evaporation-condensation.

One of the difficulties in numerically solving the Boltzmann equation comes from the varying Knudsen number, which describes the ratio of the mean free path over a typical length scale such as the domain size. When the Knudsen number is small, the collision term becomes numerically stiff. When using an explicit scheme, to guarantee the numerical stability, one has to resolve the small scales to avoid instability, and this causes tremendous computational cost. On the other hand, it is very difficult to use implicit schemes because of the nonlinear and the nonlocal nature of the collision operator.

The Chapman-Enskog expansion for the Boltzmann equation yields the compressible Euler or Navier-Stokes equations in the limit of vanishing Knudsen number. Generally speaking, numerically solving the hydrodynamic system is much more efficient, so when the Knudsen number is small, one can just solve this set of equations in lower dimension. However, in the zones where these macroscopic models break down, one comes back to solve the Boltzmann equation. This domain decomposition

*This work was partially supported by NSF grants DMS-0608720, DMS-1114546 and NSF FRG grant DMS-0757285.

[†]Department of Mathematics and Institute of Natural Sciences, Shanghai Jiao Tong University, Shanghai 200240, China; and Department of Mathematics, University of Wisconsin-Madison, Madison, WI 53706, USA (jin@math.wisc.edu)

[‡]Department of Mathematics, University of Wisconsin-Madison, Madison, WI 53706, USA (qinli@math.wisc.edu)

approach has attracted a great amount of attention [2, 3, 8, 9, 20, 23, 30, 32, 39, 40]. The main difficulty there is to determine the matching interface conditions between two different domains in which different physical models are used.

Another approach, the one we are going to pursue in this paper, is called the asymptotic preserving method. This method dated back to 90s from the last century and has been widely used in time dependent kinetic and hyperbolic system since then. This method focuses on looking for simple and cheap solver for the Boltzmann equation that can preserve asymptotic limits from the microscopic to the macroscopic models in the discrete setting, which means that the numerical solution to the Boltzmann equation should converge to that of the Euler when the Knudsen number vanishes. Compared with multiphysics domain decomposition method, this framework only solves one set of equation: the microscopic one. In the hydrodynamic regime, it becomes a robust hydrodynamic solver *automatically* without resolving the small Knudsen number or switching to the macroscopic model. As summarized by Jin [26], an AP scheme for kinetic equations should have the following features:

- it preserves the discrete analogy of the Chapman-Enskog expansion, namely, it is a suitable scheme for the kinetic equation, yet, when holding the mesh size and time step fixed and letting the Knudsen number go to zero, the scheme becomes a suitable scheme for the limiting fluid dynamic Euler equations;
- implicit collision terms can be implemented efficiently.

There are also several variations of the AP property, including weakly-AP, relaxed-AP, and strongly-AP, defined as follows (see [15] and also a recent review [27]):

- *weakly-AP*. If the data are within $O(\varepsilon)$ of the local equilibrium initially, they remain so for all future time steps;
- *relaxed-AP*. For non-equilibrium initial data, the solution will be projected to the local equilibrium beyond an initial layer (after several time steps).
- *strongly-AP*. For non-equilibrium initial data, the solution will be projected to the local equilibrium immediately at the next time step.

In general, the strongly-AP property is preferred, and was the designing principle of most of the classical AP schemes [25, 5]. The relaxed-AP was a recently introduced concept in [15] which was shown numerically to be sufficient to capture the hydrodynamic limit when the Knudsen number goes to zero. The weak-AP is often a necessary condition for the AP property, since many non-AP schemes do not satisfy this property, namely solutions initially close to the local equilibrium can move away. See discussion in [15].

Several AP schemes have recently been designed for the Boltzmann equation for one species. One approach was to use the micro-macro decomposition method [33] (see its multispecies extension in [28]), yet the main difficulty remains to design an efficient implicit collision term, which is necessary for numerical stability independent of the Knudsen number. An earlier approach introduced by Gabetta, Pareschi and Toscani uses the truncated Wild Sum [17]. For a simple BGK model it was realized by Coron and Perthame in [7] that an implicit BGK operator can be integrated explicitly, using the basic conservation properties of the BGK operator. Utilizing this property, Filbet and Jin introduced the BGK penalization method for the Boltzmann collision operator [15]. The main idea is to subtracting the Boltzmann operator by a BGK operator, and then add the BGK operator back. Only the latter BGK operator is treated implicitly, while the complicated Boltzmann operator is solved explicitly. The entire scheme is implemented explicitly, yet the numerical stability is independent of the Knudsen

number and the relaxed AP property was achieved (which was verified numerically). This BGK penalization idea, in the space homogeneous case, agrees with the Wild Sum approach [17], but for space inhomogeneous case, they differ and one can find a different implementation using the exponential Runge-Kutta method, see Dimarco and Pareschi [12], resulting a strongly AP scheme with positivity. A rigorous justification of the AP property of this methodology for hyperbolic systems with stiff relaxation was carried out recently in [16]. The BGK penalization method has also been extended to Fokker-Planck-Landau equation [29], the quantum Boltzmann equation [14], and the quantum Fokker-Planck-Landau equation [24].

In this article, we generalize the BGK-penalization idea of Filbet-Jin to the multispecies Boltzmann equation. Several new difficulties arise here. First there are several possible choices of the local Maxwellian and one has to determine the one that suits our needs. Secondly, to justify various AP properties one needs to prove that the velocities and temperatures of different species equilibrate, a property one does not encounter for the single species Boltzmann equation. Finally we also demonstrate that this method can also be used for gas mixtures with disparate masses, which arises in ion-electron evolution problem in plasma [21, 4, 38].

This paper is organized as follows: we will describe the Boltzmann equation for the multispecies system and one of its related BGK models in section 2, including their theoretical properties. In section 3, we will give details of the numerical scheme. This is followed by section 4 where we prove various AP properties of the scheme. In section 5, we discuss the disparate masses system. In section 6, we show several numerical examples.

2 The Multispecies Models

2.1 The multispecies Boltzmann Equation

The Boltzmann equation describes the evolution of the density distribution of rarefied gases. The Boltzmann equation for the multispecies system is given by [13]:

$$\partial_t f_i + v \cdot \nabla_x f_i = Q_i(f, f), \quad t \geq 0, \quad (x, v) \in \mathbb{R}^d \times \mathbb{R}^d, \quad (2.1)$$

with

$$Q_i(f, f) = \sum_{k=1}^N Q_{ik}(f, f), \quad (2.2a)$$

$$Q_{ik}(f, f)(v) = \int_{B_+} \int_{\mathbb{R}^d} (f'_i f'_{k*} - f_i f_{k*}) B_{ik}(|v - v_*|, \Omega) dv_* d\Omega, \quad (2.2b)$$

where for each species i , Q_i stands for its collision, which is the summation of Q_{ik} , the collision between the i th and the k th species, B_{ik} is the collision kernel, which in general depends on the pre-collisional relative velocity $g = v - v_*$, and a unit vector Ω . For Maxwell molecule, the collision kernel only depends on the angle $\omega = \arccos \frac{g \cdot \Omega}{|g|}$, i.e. $B_{ik} = B_{ik}(\omega)$; f'_i and f'_{k*} are distributions for species i and k respectively at the post-collisional velocities v' and v'_* , which satisfy:

$$v' = v - \frac{2\mu_{ik}}{m_i} (g \cdot \Omega) \Omega, \quad (2.3a)$$

$$v'_* = v_* + \frac{2\mu_{ik}}{m_k} (g \cdot \Omega) \Omega, \quad (2.3b)$$

with $\mu_{ik} = \frac{m_i m_k}{m_i + m_k}$ being the reduced mass and m_i, m_k being the mass for species i and k respectively. Deduction of the velocity change (2.3) is based on momentum and energy conservations:

$$\begin{aligned} m_i v + m_k v_* &= m_i v' + m_k v'_*, \\ m_i |v|^2 + m_k |v_*|^2 &= m_i |v'|^2 + m_k |v'_*|^2. \end{aligned}$$

2.2 Properties of the multispecies Boltzmann equation

We define the macroscopic quantities for species i : n_i is the number density; ρ_i is the mass density; u_i is the average velocity; E_i is the total energy; e_i is the internal energy per particle; T_i is the temperature; P_i is the stress tensor; and q_i is the flux vector, given by:

$$\begin{aligned}
n_i &= \int f_i dv_i, & \rho_i &= m_i n_i, \\
\rho_i u_i &= m_i \int v f_i dv, \\
E_i &= \frac{1}{2} \rho_i u_i^2 + n_i e_i = \frac{1}{2} m_i \int |v|^2 f_i dv, \\
e_i &= \frac{d}{2} T_i = \frac{m_i}{2n_i} \int f_i |v - u_i|^2 dv, \\
P_i &= \int (v - u_i) \otimes (v - u_i) f_i dv, \\
q_i &= \frac{1}{2} m_i \int (v - u_i) |v - u_i|^2 f_i dv.
\end{aligned} \tag{2.4}$$

We also define global quantities for the mixture: the total mass density ρ , the number density n , the mean velocity \bar{u} , the total energy E , the internal energy $n\bar{e}$ and the mean temperature $\bar{T} = \frac{2\bar{e}}{d}$:

$$\begin{aligned}
\rho &= \sum_i \rho_i, & n &= \sum_i n_i, \\
\rho \bar{u} &= \sum_i \rho_i u_i, \\
E &= \frac{d}{2} n \bar{T} + \frac{\rho}{2} |\bar{u}|^2 = \sum_i E_i.
\end{aligned} \tag{2.5}$$

2.2.1 Conservation

In the gas mixture system, for each species, the mass is conserved, but not the momentum and energy. Namely, taking the moments of the collision term, one multiplies it with $\phi = m_i [1, v, \frac{1}{2}|v|^2]$ and integrates in velocity and gets:

$$\begin{aligned}
\langle m_i Q_i \rangle &= \int m_i Q_i(f) dv = 0, \\
\langle m_i v Q_i \rangle &= \int m_i v Q_i(f) dv = \sum_{k=1}^n 2\mu_{ik} \chi_{ik} n_i n_k [u_k - u_i], \\
\langle \frac{1}{2} m_i v^2 Q_i \rangle &= \int \frac{m_i}{2} |v|^2 Q_i(f) dv \\
&= \sum_{k=1}^n 2m_i \chi_{ik} n_i n_k \left[\left(\frac{\mu_{ik}}{m_i} \right)^2 \left(|u_k - u_i|^2 + 2 \frac{e_k}{m_k} + 2 \frac{e_i}{m_i} \right) + \frac{\mu_{ik}}{m_i} \left((u_k - u_i) \cdot u_i - 2 \frac{e_i}{m_i} \right) \right],
\end{aligned}$$

where $\chi_{ik} = \int (\cos \omega)^2 B_{ik}(\omega) d\omega$ for Maxwell molecules. The details can be found in [1].

Based on these formulas, when taking moments of the Boltzmann equation, we get evolution of the macro quantities (taking 1D Maxwell molecule for example):

$$\begin{aligned}
\partial_t \rho_i + \partial_x(\rho_i u_i) &= \langle m_i Q_i \rangle = 0, \quad \text{or} \quad \partial_t n_i + \partial_x(n_i u_i) = 0, \\
\partial_t(\rho_i u_i) + \partial_x(P_i + \rho_i u_i^2) &= \langle m_i v Q_i \rangle = \frac{1}{\varepsilon} \sum_k 2B_{ik} n_i n_k \mu_{ik} [u_k - u_i], \\
\partial_t E_i + \partial_x(E_i u_i + P_i u_i + q_i) &= \langle \frac{1}{2} m_i |v|^2 Q_i \rangle = \frac{1}{\varepsilon} \sum_k 2B_{ik} n_i n_k \left(\frac{\mu_{ik}^2}{m_i m_k} \right) (a + b),
\end{aligned} \tag{2.6}$$

where $a = (m_k u_k + m_i u_i) \cdot (u_k - u_i)$, $b = 2(e_k - e_i)$. However, the total momentum and total energy are still conserved:

$$\begin{aligned}
\partial_t \rho + \partial_x(\rho \bar{u}) &= 0, \\
\partial_t(\rho \bar{u}) + \partial_x\left(\sum_i P_i + \sum_i \rho_i u_i^2\right) &= \frac{1}{\varepsilon} \sum_i \langle m_i v_i Q_i \rangle = 0, \\
\partial_t E + \partial_x\left(\sum_i E_i u_i + \sum_i P_i u_i + \sum_i q_i\right) &= \frac{1}{\varepsilon} \sum_i \langle \frac{1}{2} m_i v_i^2 Q_i \rangle = 0.
\end{aligned} \tag{2.7}$$

2.2.2 The local Maxwellian

The local equilibrium is reached when the gaining part and losing part of collision for each species i balance out, namely $Q_i(f) = 0$ for each i . It is given by:

$$f_i = \bar{M}_i = n_i \left(\frac{m_i}{2\pi\bar{T}} \right)^{d/2} e^{-\frac{m_i |v - \bar{u}|^2}{2\bar{T}}}, \tag{2.8}$$

where \bar{T} is the mean temperature and \bar{u} is mean velocity defined in (2.5). We call this Maxwellian the ‘‘unified Maxwellian’’ because the macro quantities are given by those for the entire system instead of those for the single species.

2.2.3 The Euler limit

Expanding f_i around the unified Maxwellian (2.8), the standard Chapman-Enskog expansion shows that at the local equilibrium, the collision term vanishes, and the system gets to its Euler limit [1]:

$$\begin{aligned}
\partial_t \rho_i + \nabla \cdot (\rho_i \bar{u}) &= 0, \\
\partial_t(\rho \bar{u}) + \nabla \cdot (\rho \bar{u} \otimes \bar{u} + \rho \bar{T} \mathbb{I}) &= 0, \\
\partial_t E + \nabla \cdot ((E + \rho \bar{T}) \bar{u}) &= 0.
\end{aligned} \tag{2.9}$$

2.3 A BGK model

The BGK operator is a classical approximation for collision term. There are several BGK models, but most of them either suffer from the loss of positivity [18], or fail to satisfy the indifferentiability principle [22, 37, 19]. Positivity guarantees that the distribution function is always positive, and indifferentiability requires that when different species share the same mass, equations of the system should be consistent with the single species Boltzmann equation. We choose the BGK model proposed by Andries, Aoki and Perthame [1], the one that guarantees the indifferentiability principle and positivity.

The model reads:

$$\partial_t f_i + v \cdot \nabla_x f_i = \frac{\nu_i}{\varepsilon} (\bar{M}_i - f_i), \tag{2.10}$$

with ν_i being collision frequency and \widetilde{M}_i being a Maxwellian:

$$\begin{aligned}\nu_i &= \sum_k n_k \chi_{ik}, \\ \widetilde{M}_i &= n_i \left(\frac{m_i}{2\pi\widetilde{T}_i} \right)^{d/2} e^{-\frac{m_i|\xi-\widetilde{u}_i|^2}{2\widetilde{T}_i}},\end{aligned}\tag{2.11}$$

where the macro quantities for \widetilde{M} are given by:

$$\nu_i \widetilde{u}_i - \nu_i u_i = \langle v Q_i \rangle = \frac{1}{m_i} \sum_{k=1}^n 2\mu_{ik} \chi_{ik} n_i n_k [u_k - u_i],\tag{2.12a}$$

$$\begin{aligned}\nu_i \widetilde{E}_i - \nu_i E_i &= \langle \frac{1}{2} m_i v^2 Q_i \rangle \\ &= \sum_{k=1}^n 2m_i \chi_{ik} n_i n_k \left[\left(\frac{\mu_{ik}}{m_i} \right)^2 \left(|u_k - u_i|^2 + 2\frac{e_k}{m_k} + 2\frac{e_i}{m_i} \right) + \frac{\mu_{ik}}{m_i} \left((u_k - u_i) \cdot u_i - 2\frac{e_i}{m_i} \right) \right].\end{aligned}\tag{2.12b}$$

$\widetilde{T}_i = (2\widetilde{E}_i - \rho_i \widetilde{u}_i^2) / (n_i d)$ as usual. The way \widetilde{M} is defined is to capture the moments of the collision Q . Note that the right hand side of equation (2.12a) is just a linear operator of u . For later reference, we define a matrix \mathbb{L} by:

$$(\mathbb{L})_{ij} = \begin{cases} 2\mu_{ij} \chi_{ij} n_i n_j, & i \neq j, \\ \sum_k -2\mu_{ik} \chi_{ik} n_i n_k, & i = j. \end{cases}\tag{2.13}$$

Apparently, \mathbb{L} is a symmetric matrix with each row summing up to 0, and all elements not on the diagonal are positive. Since \mathbb{L} is a symmetric weakly diagonally dominant matrix, thus it is semi-negative definite, i.e. all its eigenvalues are non-positive. Equation (2.12a) turns out to be $\nu_i \widetilde{u}_i - \nu_i u_i = \frac{1}{m_i} (\mathbb{L}u)_i$. For later convenience, we also define the following notation: for any non-singular matrix \mathbb{A} , we use $\Lambda(\mathbb{A})$ to denote its spectral radius:

$$\Lambda(\mathbb{A}) = \sup_i (|\lambda_i(\mathbb{A})|),\tag{2.14}$$

where $\lambda_i(\mathbb{A})$ are eigenvalues of \mathbb{A} .

Similar results can be carried out for e : when u is known, the right hand side of (2.12b) is linear on e .

Remark 1. Equation (2.12a) holds componentwise for vector u_i so \mathbb{L} should be acted on each component of u_i .

We also mention another type of Maxwellian, which is defined by species' own macro quantities u_i and T_i . We call it the ‘‘species Maxwellian’’:

$$M_i = n_i \left(\frac{m_i}{2\pi T_i} \right)^{d/2} e^{-\frac{m_i|\xi-u_i|^2}{2T_i}}.\tag{2.15}$$

Remark 2. $M_i - f_i$ could not be used as a BGK operator. In the multispecies system, one has to introduce some mechanism into the collision term that captures the influence between species. $M_i - f_i$ gives no communication between the species, so it cannot be used to express the multispecies collision.

3 An AP Scheme for the multispecies Boltzmann equation

In this chapter, we derive our AP scheme for the multispecies Boltzmann equation. Our idea is based on BGK-penalization method proposed by Filbet and Jin [15].

3.1 The time discretization

Here we adopt the same strategy and write our scheme as:

$$\frac{f_i^{l+1} - f_i^l}{\Delta t} + v \cdot \nabla_x f_i^l = \frac{Q_i^l(f) - P_i^l(f)}{\varepsilon} + \frac{P_i^{l+1}(f)}{\varepsilon}. \quad (3.1)$$

The superscript l stands for the time step. And P is chosen to be the leading order expansion of Q :

$$P = \beta(\bar{M} - f). \quad (3.2)$$

A simple algebraic manipulation on (3.1) gives:

$$f_i^{l+1} = \frac{\varepsilon f_i^l + \Delta t(Q_i^l - \beta^l(\bar{M}_i^l - f_i^l)) - \varepsilon \Delta t v \cdot \nabla_x f_i^l + \beta^{l+1} \Delta t \bar{M}_i^{l+1}}{\varepsilon + \beta^{l+1} \Delta t}.$$

The three macroscopic quantities that define \bar{M} come from solving the Euler equations for the entire system described in details below.

3.2 The computation of \bar{M}^{l+1}

Numerically integrating system (2.7), one gets:

$$\begin{aligned} n_i^{l+1} &= n_i^l - \Delta t \int v \cdot \nabla_x f_i^l dv, \\ (\rho \bar{u})^{l+1} &= (\rho \bar{u})^l - \Delta t \sum_i m_i \int v \otimes v \cdot \nabla_x f_i^l dv, \\ E^{l+1} &= E^l - \Delta t \sum_i \int \frac{m_i}{2} |v|^2 v \cdot \nabla_x f_i^l dv, \\ \bar{T}^{l+1} &= \frac{2E^{l+1} - (\rho \bar{u}^2)^{l+1}}{n^{l+1}}, \end{aligned}$$

where the flux term is computed in section 3.4. Now \bar{M}^{l+1} is given by (2.8).

3.3 The collision term Q

We use the spectral method introduced in [36] to compute the collision term Q_i . Use a ball $B(0, S)$ to approximate a compactly supported distribution f . Then we periodize f on $v \in [-L, L]^d$ with $L \geq (3 + \sqrt{2})S$. L is chosen much larger than S to avoid non-physical collision at different periods of periodized f . Define the Fourier Transform as:

$$\begin{aligned} \hat{f}(k; x) &= \int f(v; x) e^{-ikv} dv, \\ f(v; x) &= \frac{1}{(2L)^d} \sum_k \hat{f}(k; x) e^{ikv}. \end{aligned}$$

Plugging into the collision term (2.2b):

$$Q_{ik} = \int \int B_{ik} [f'_i f'_{k^*} - f_i f_{k^*}] dv_k dn \equiv Q_{ik}^+ - Q_{ik}^-,$$

with

$$Q_{ik}^+ = \int \int B_{ik} \left(\frac{1}{2L} \right)^{2d} \left[\sum_p \sum_q \hat{f}_i(p; x) e^{ipv'} \hat{f}_k(q; x) e^{iqv_*'} \right] dv_* dn,$$

$$Q_{ik}^- = \int \int B_{ik} \left(\frac{1}{2L} \right)^{2d} \left[\sum_p \sum_q \hat{f}_i(p; x) e^{ipv} \hat{f}_k(q; x) e^{iqv_*} \right] dv_* dn.$$

Taking the 1D Maxwell molecule for example, the post-collisional velocities are

$$v' = v - \frac{2m_k}{m_i + m_k} (v - v_*) = \frac{m_i - m_k}{m_i + m_k} v + \frac{2m_k}{m_i + m_k} v_*,$$

$$v_*' = v + \frac{m_i - m_k}{m_i + m_k} (v - v_*) = \frac{2m_i}{m_i + m_k} v - \frac{m_i - m_k}{m_i + m_k} v_*.$$

Plugging in Q_{ik}^+ , one gets:

$$Q_{ik}^+ = \frac{B_{ik}}{(2L)^{2d}} \sum_{p,q} \hat{f}_i^p \hat{f}_k^q e^{[i(\frac{m_i - m_k}{m_i + m_k} p + \frac{2m_i}{m_i + m_k} q)v]} \int e^{[i(\frac{2m_k}{m_i + m_k} p - \frac{m_i - m_k}{m_i + m_k} q)v_*]} dv_*.$$

One can also write Q_{ik}^+ as a summation of its Fourier modes $Q_{ik}^+ = (\frac{1}{2L})^d \sum_l \hat{Q}_{ik}^{l+} e^{ilv}$ where

$$\begin{aligned} \hat{Q}_{ik}^{l+} &= \int Q_{ik}^+ e^{-ilv} dv \\ &= \frac{B_{ik}}{(2L)^{2d}} \sum_{p,q} \hat{f}_i^p \hat{f}_k^q \int e^{i(\frac{m_i - m_k}{m_i + m_k} p + \frac{2m_i}{m_i + m_k} q - l)v} dv \int e^{i(\frac{2m_k}{m_i + m_k} p - \frac{m_i - m_k}{m_i + m_k} q)v_*} dv_* \\ &= B_{ik} \sum_{p,q} \hat{f}_i^p \hat{f}_k^q \text{sinc}(a) \text{sinc}(b), \end{aligned}$$

where $a = (\frac{m_i - m_k}{m_i + m_k} p + \frac{2m_i}{m_i + m_k} q - l)L$, and $b = (\frac{2m_k}{m_i + m_k} p - \frac{m_i - m_k}{m_i + m_k} q)L$. The FFT and the inverse FFT are used to speed up the computation.

The computation for Q_{ik}^- is much simpler in this special case: $Q_{ik}^- = f_i \int B_{ik} f_k dv_k = f_i n_k B_{ik}$.

After getting all Q_{ik} , $Q_i = \sum_k Q_{ik}$.

3.4 The flux term $v \cdot \nabla_x f_i$

Here we show computation in 1D. Use $v \partial_x f_{i,j}$ to denote the flux term for species i for grid point x_j . A shock-capturing finite volume method we use is [34]:

$$v \partial_x f_{i,j} = \nu (f_{i,j_1}^l - f_{i,j_1-1}^l) - \frac{1}{2} \nu (\text{sgn}(\nu) - \nu) (h \sigma_{i,j_1} - h \sigma_{i,j_1-1}), \quad (3.3)$$

where $\nu = \frac{v}{h}$, h is mesh size. j_1 is chosen to be j for $v > 0$ and $j+1$ for $v < 0$. $\sigma_{i,j} = \frac{f_{i,j+1} - f_{i,j}}{h} \phi_{i,j}$ where $\phi_{i,j}$ is the slope limiter. For the van Leer limiter, it takes value as $\phi(\theta) = \frac{\theta + |\theta|}{\theta + 1}$ and $\theta_{i,j} = \frac{f_{i,j} - f_{i,j-1}}{f_{i,j+1} - f_{i,j}}$ reflects smoothness around grid point x_j .

The computation for the flux term in higher dimension can also be found in [34].

4 The AP Property of the Time Discretization

The time discrete scheme (3.1) is written as:

$$\frac{f_i^{l+1} - f_i^l}{\Delta t} + v \cdot \nabla_x f_i^l = \frac{Q_i^l - \beta(\overline{M}_i^l - f_i^l)}{\varepsilon} + \frac{\beta(\overline{M}_i^{l+1} - f_i^{l+1})}{\varepsilon}. \quad (4.1)$$

We will show below that this method is weakly-AP for general Boltzmann collision operator, and relaxed-AP for the BGK model given in section 2.3. Below we always assume that $\Delta t \gg \varepsilon$, and we use the linear operator \mathbb{L} defined in (2.13), $\Lambda(\mathbb{A})$ in (2.14), and denote \mathbb{I} as the identity matrix. We also define:

$$\delta u_i^l = u_i^l - \bar{u}^l, \quad \delta T_i^l = T_i^l - \bar{T}^l, \quad (4.2)$$

and

$$\varrho = \begin{bmatrix} \rho_1, 0, \dots, 0 \\ 0, \rho_2, \dots, \vdots \\ \vdots, \dots, \dots, \vdots \\ 0, \dots, \dots, \rho_N \end{bmatrix} \quad (4.3)$$

4.1 Weakly-AP

Lemma 1. If $\delta u_i^l = O(\varepsilon)$ and $\delta T_i^l = O(\varepsilon)$ for $\forall i$, then $\delta u_i^{l+1} = O(\varepsilon)$ and $\delta T_i^{l+1} = O(\varepsilon)$.

Proof. Rewrite scheme (4.1) as:

$$f_i^{l+1} - \bar{M}_i^{l+1} = \frac{\varepsilon(-\bar{M}_i^{l+1} + \bar{M}_i^l) - \varepsilon \Delta t v \cdot \nabla_x f_i^l}{\varepsilon + \beta \Delta t} + \frac{\Delta t Q_i^l}{\varepsilon + \beta \Delta t} - (\bar{M}_i^l - f_i^l). \quad (4.4)$$

Take the first moment on both sides. On the left hand side, one gets $(\rho_i u_i)^{l+1} - (\rho_i \bar{u})^{l+1}$, while on the right hand side, the first term is $O(\varepsilon)$. The second term gives:

$$\begin{aligned} \frac{\Delta t}{\varepsilon + \beta \Delta t} \langle m_i v Q_i^l \rangle &= \frac{\Delta t}{\varepsilon + \beta \Delta t} \sum_k 2\chi_{ik} \mu_{ik} n_i n_k [u_k^l - u_i^l] \\ &= \frac{\Delta t}{\varepsilon + \beta \Delta t} \sum_k 2\chi_{ik} \mu_{ik} n_i n_k (\delta u_k^l - \delta u_i^l) = O(\varepsilon). \end{aligned}$$

The third term gives:

$$\langle m_i v (\bar{M}_i^l - f_i^l) \rangle = \rho_i (\bar{u}^l - u_i^l) = O(\varepsilon).$$

So the entire right hand side is of $O(\varepsilon)$, thus the term on the left hand side, $(\rho_i u_i)^{l+1} - (\rho_i \bar{u})^{l+1} = O(\varepsilon)$, i.e. $\delta u_i^{l+1} = O(\varepsilon)$. Similar analysis can be carried out for T . \square

Theorem 1. The method is weakly-AP; namely, if $\bar{M}_i^l - f_i^l = O(\varepsilon)$, then $\bar{M}_i^{l+1} - f_i^{l+1} = O(\varepsilon)$.

Proof. Since $\bar{M}_i^l - f_i^l = O(\varepsilon)$, both $P_i(f^l)$ and $Q_i(f^l)$ are of $O(\varepsilon)$. Plugging back into the scheme (4.1), one gets $f_i^{l+1} - \bar{M}_i^{l+1} = O(\varepsilon)$. \square

4.2 Relaxed-AP

Lemma 2. When $\Delta t \ll 1$, in the limit of $\varepsilon \rightarrow 0$, if $\beta > \frac{1}{2}\Lambda(\varrho^{-1}\mathbb{L})$, then there $\exists N_t$, such that $\forall l > N_t$, $\delta u^l = O(\varepsilon)$.

Proof. We prove the scheme for 1D case. The proof for higher dimension can be carried out easily. One can take moments of the numerical scheme (4.1):

$$\begin{aligned} \frac{(\rho u)^{l+1} - (\rho u)^l}{\Delta t} + \partial_x \int v^2 m f^l dv &= \frac{1}{\varepsilon} (\mathbb{L}u^l + \beta \varrho^l \delta u^l - \beta \varrho^{l+1} \delta u^{l+1}), \\ \Rightarrow (\varepsilon + \beta \Delta t) \varrho^{l+1} \delta u^{l+1} &= \left((\varepsilon + \beta \Delta t) \varrho^l + \Delta t \mathbb{L} \right) \delta u^l + \varepsilon \left((\rho \bar{u})^l - (\rho \bar{u})^{l+1} \right) - \varepsilon \Delta t \partial_x \int v^2 m f^l dv, \\ \Rightarrow (\varepsilon + \beta \Delta t) \varrho^{l+1} \delta u^{l+1} &= \left[(\varepsilon + \beta \Delta t) \left(\varrho^{l+1} + O(\Delta t) \right) + \Delta t \mathbb{L} \right] \delta u^l + O(\varepsilon), \end{aligned}$$

where $\mathbb{L}\bar{u} = 0$ and $\varrho^{l+1} = \varrho^l + O(\Delta t)$ is used.

After some simple algebra, one can rewrite the previous equation as:

$$\delta u^{l+1} = \left[\mathbb{I} + \beta^{-1}(\varrho^{l+1})^{-1}\mathbb{L} + O(\Delta t) \right] \delta u^l + O(\varepsilon)$$

Define α_u as:

$$\alpha_u = \left[\mathbb{I} + \beta^{-1}(\varrho^{l+1})^{-1}\mathbb{L} + O(\Delta t) \right]. \quad (4.5)$$

Since the eigenvalues for \mathbb{L} are non-positive, if one chooses $\beta > \frac{1}{2}\Lambda(\varrho^{-1}\mathbb{L})$, given small enough Δt , $|\Lambda(\alpha_u)| < 1$, thus in the limit of $\varepsilon \rightarrow 1$, δu would decrease till $O(\varepsilon)$, and we get our conclusion. Similar idea can also be found in [15]. \square

The same analysis can be carried out for T .

Theorem 2. For $\varepsilon \ll 1$, $\exists N_t$ such that $\forall l > N_t$, $M_i^l - \bar{M}_i^l = O(\varepsilon)$, and $\widetilde{M}_i^l - \bar{M}_i^l = O(\varepsilon)$.

Proof. It is a straightforward conclusion from the lemma above, and from the definition for \widetilde{M} in (2.11). \square

Remark 3. Up to now, we have shown that M_i approaches to \bar{M}_i for general Boltzmann collision operator. Rearranging scheme (4.1), one gets:

$$f^{l+1} - \bar{M}^{l+1} = \frac{(\varepsilon + \beta\Delta t)(f^l - \bar{M}^l) + \Delta t Q^l}{\varepsilon + \beta\Delta t} + \frac{\varepsilon(\bar{M}^l - \bar{M}^{l+1}) - \varepsilon\Delta t v \cdot \nabla_x f^l}{\varepsilon + \beta\Delta t}. \quad (4.6)$$

The second term is of $O(\varepsilon)$. So, one can get relaxed-AP only if Q being negative whenever $f - \bar{M}$ is positive can be showed. We can prove this for limited form of Q , say the BGK operator introduced in section 2.3. Later in section 6 we will show that numerically the scheme is relaxed-AP for the collision defined in (2.2).

Theorem 3. The scheme is relaxed-AP for BGK operator $Q = \nu(\widetilde{M} - f)$.

Proof. Plug in the definition for Q , (4.6) writes:

$$\begin{aligned} f^{l+1} - \bar{M}^{l+1} &= \frac{\varepsilon + \beta\Delta t - \nu\Delta t}{\varepsilon + \beta\Delta t} (f^l - \bar{M}^l) + \frac{\nu\Delta t(\widetilde{M}^l - \bar{M}^l)}{\varepsilon + \beta\Delta t} + O(\varepsilon) \\ &= \frac{\varepsilon + \beta\Delta t - \nu\Delta t}{\varepsilon + \beta\Delta t} (f^l - \bar{M}^l) + O(\varepsilon) \end{aligned}$$

The second equality comes from Theorem 2. Define:

$$\alpha_M = \frac{\varepsilon + \beta\Delta t - \nu\Delta t}{\varepsilon + \beta\Delta t} \quad (4.7)$$

and we call it the convergent rate to the unified Maxwellian \bar{M} . In the limit of $\varepsilon \rightarrow 0$, if one has $\beta > \frac{\nu}{2}$, then $|\alpha_M| < 1$, thus $|f - \bar{M}|$ keeps diminishing till reaching to $O(\varepsilon)$, and we get relaxed-AP. \square

5 Disparate Masses

This section is for the system of gas mixture with disparate masses in homogeneous space. The mathematical problem was first pointed out by Grad [21], and has attracted great interests since then. The fundamental example is plasma, for which, the basic derivation can be found in [4, 38]. For these systems, it is the different time scalings for different species to reach to the equilibrium that make the problem difficult. Generally speaking, the light species should be able to get to the equilibrium faster. Analyses of the scaling of the collision operators have been done both based on postulate physical consideration [31, 6] and using formal derivation [10, 11].

5.1 Theoretical rescaling analysis

We will make use of the rescaling used in [10, 11] where they get the scaling ratio of collision for heavy particle over that of the light one is $O(\varepsilon)$, $\varepsilon = \sqrt{m_L/m_H}$ and the sub index H and L are for the heavy and the light species respectively. The system is written as:

$$\begin{cases} \partial_t f_H = Q_H = Q_{HH} + Q_{HL} = \int (f'_H f'_{H*} - f_H f_{H*}) dv_{H*} + \int (f'_H f'_L - f_H f_L) dv_L, \\ \partial_t f_L = Q_L = Q_{LL} + Q_{LH} = \int (f'_L f'_{L*} - f_L f_{L*}) dv_{L*} + \int (f'_H f'_L - f_H f_L) dv_H. \end{cases} \quad (5.1)$$

Considering that f_H is much narrower than f_L given that the two species have similar temperature at initial time (Figure 1 gives an idea on how the two distribution functions look like at the beginning), one needs to define $\tilde{v} = \frac{v}{\varepsilon}$ and $\tilde{f}_H(v) = f_H(\frac{v}{\varepsilon})$ to stretch f_H to a function that has similar variance as f_L . We will skip the details and only adopt the results from [10, 11] where the authors get

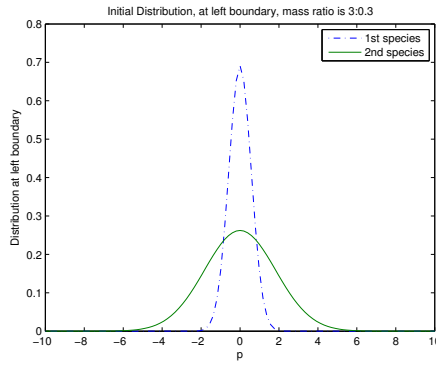


Figure 1: Distribution for heavy species is much narrower than that of the light species

$Q_{HH}/Q_{HL}/Q_{LH}/Q_{LL} = O(\varepsilon)/O(\varepsilon)/1/1$, which means that $Q_H/Q_L = O(\varepsilon)$. For convenience, we write both Q_H and Q_L as $O(1)$ term, then the system turns out to be:

$$\begin{cases} \partial_t f_H = \frac{\varepsilon}{\tau} Q_H, \\ \partial_t f_L = \frac{1}{\tau} Q_L, \end{cases} \quad (5.2)$$

where τ is the time scaling parameter.

Remark 4. The inhomogeneous problem gets even harder to deal with if different species have different spatial rescaling coefficients. Numerically it makes little difference: one just needs to add the flux term $v \cdot \nabla_x f$ term to the homogeneous scheme.

5.2 The Numerical Scheme

In order to capture the long time behavior, the scheme we design to solve (5.2) is:

$$\frac{f_H^{l+1} - f_H^l}{\Delta t} = \frac{1}{\tau} (\varepsilon(Q_H^l - \beta(M_H^l - f_H^l))) + \frac{\beta\varepsilon}{\tau} (M_H^{l+1} - f_H^{l+1}), \quad (5.3a)$$

$$\frac{f_L^{l+1} - f_L^l}{\Delta t} = \frac{1}{\tau} (Q_L^l - \beta(M_L^l - f_L^l)) + \frac{\beta}{\tau} (M_L^{l+1} - f_L^{l+1}), \quad (5.3b)$$

where $\beta = O(1)$.

Theorem 4. This scheme gives a correct discretization to the problem in both time scales: $O(\frac{1}{\varepsilon})$ and $O(\frac{1}{\varepsilon^2})$.

- at $\tau = O(\frac{1}{\varepsilon})$ time scale, the scheme is first order consistent to $\partial_t f_H = Q_H$, and f_L^l is an $O(\varepsilon)$ approximation of \overline{M}_L ;
- at $\tau = O(\frac{1}{\varepsilon^2})$ time scale, both f_H^l and f_L^l are within $O(\varepsilon)$ of the unified Maxwellians \overline{M}_H and \overline{M}_L respectively.

Proof. To prove the second statement:

At this time scale, $\tau = O(\varepsilon^2)$, the system turns out to be:

$$\begin{cases} \partial_t f_H = \frac{1}{\varepsilon} Q_H, \\ \partial_t f_L = \frac{1}{\varepsilon^2} Q_L. \end{cases}$$

By the same arguments as in the previous sections, one gets:

$$\begin{cases} f_H - \overline{M}_H = O(\varepsilon), \\ f_L - \overline{M}_L = O(\varepsilon^2). \end{cases}$$

To prove the first statement:

At this time scale, $\tau = O(\varepsilon)$, system (5.3) can be written as:

$$\begin{cases} \partial_t f_H = Q_H, \\ \partial_t f_L = \frac{1}{\varepsilon} Q_L. \end{cases}$$

The scheme still gives $f_L^l \rightarrow \overline{M}_L^l$. One just needs to show that the scheme gives a correct discretization of the equation for f_H too. Write (5.3a) as (set $\tau = \varepsilon$):

$$\frac{f_H^{l+1} - f_H^l}{\Delta t} = Q_H^l - \beta(M_H^l - f_H^l) + \beta(M_H^{l+1} - f_H^{l+1}).$$

Rearrange it, one gets:

$$\frac{f_H^{l+1} - f_H^l}{\Delta t} = Q_H^l - \frac{\beta\Delta t}{1 + \beta\Delta t} Q_H^l + \frac{\beta}{1 + \beta\Delta t} (M_H^{l+1} - M_H^l).$$

The second and the third terms on the right are both of order Δt , i.e. the scheme gives a first order discretization to $\partial_t f_H = Q_H$. \square

6 Numerical Examples

For comparison, the examples chosen are similar to those in [28]. We also perturb the data on the macro quantities. For all the examples below: when ε is not very small so that solving the Boltzmann equation is still possible by using the basic explicit scheme with resolved mesh, we compare numerical results of the new AP scheme with the forward Euler scheme, and when ε is unbearably small for the forward Euler, we compare results given by the new scheme with its Euler limit. To solve the Euler equations, we used the CLAWPACK Euler solver [35].

6.1 A Stationary Shock

In this example, we show numerical solution to a Riemann problem of two species. The analytical solution to the Euler equation is a shock with zero speed. Here the subscript stands for data to different species.

$$\begin{cases} m_1 = 1, m_2 = 1.5, n_1 = n_2 = 1, u_1 = 1.8, u_2 = 1.3, T_1 = T_2 = 0.325, & \text{if } x < 0; \\ m_1 = 1, m_2 = 1.5, n_1 = n_2 = 1.401869, u_1 = u_2 = 1.07, T_1 = T_2 = 0.8605, & \text{if } x > 0. \end{cases}$$

The initial distribution for f is given by summation of two Gaussian functions, so it is far away from the unified Maxwellian \bar{M} ,

$$f(t=0) = \sum_{i=1}^2 A_i e^{-B_i(v-C_i)^2}, \quad (6.1)$$

where

$$B_1 = B_2 = \frac{\rho}{4E - 2\rho u^2(1 + \kappa^2)}, \quad A_1 = A_2 = \frac{n}{2} \sqrt{\frac{B}{\pi}} \quad \text{and} \quad C_1 - u = u - C_2 = \kappa u. \quad (6.2)$$

In the numerical experiment, we choose $\kappa = 0.2$. $\Delta x = 10^{-2}$ and Δt is chosen to satisfy the CFL condition: 10^{-3} in our simulation. Numerically we check the followings: 1. Does the new AP scheme give the Euler limit when ε goes to zero; 2. Does the AP scheme match well with the forward Euler method with relatively fine mesh when ε is big. We first show in Figure 2 that as ε goes to zero, the numerical solution converges to the Euler limit, to be specific, the stationary shock in this case. In Figure 3, we show that the AP scheme matches very well with the numerical results given by the forward Euler method for $\varepsilon = 10^{-1}$. Then we show in Figure 4, that given an initial data far away from the unified Maxwellian, f converges to \bar{M} quickly with $\varepsilon = 10^{-5}$. This verifies that the scheme is relaxed-AP numerically. Figure 5 shows that smaller ε gives faster convergence to the equilibrium state for velocities.

6.2 The Sod Problem

In this example, we compute the Sod problem. Initial data is given by:

$$\begin{cases} m_1 = m_2 = 1, n_1 = 1, n_2 = 1.2, u_1 = 0.6, u_2 = -0.5, T_1 = T_2 = 0.709, & \text{if } x < 0; \\ m_1 = m_2 = 1, n_1 = 0.125, n_2 = 0.2, u_1 = -0.2, u_2 = 0.125, T_1 = T_2 = 0.075, & \text{if } x > 0. \end{cases}$$

The initial distribution is given by the same formulas in (6.1) and (6.2) with $\kappa = 0.2$. For all ε , choose $\Delta x = 10^{-2}$ and $\Delta t = 10^{-3}$. In this problem, $m_1 = m_2$, so we first show the numerical indifferentiability in Figure 6, that is: computing the problem as a multispecies system gives the same result as computing the single-species Boltzmann equation. In Figure 7, we show that as ε goes to zero, the numerical solution converges to the Euler limit. For ε as big as 10^{-1} and 10^{-2} , we compare the results with those of the forward Euler with a fine mesh. They match well as shown in Figure 8. In Figure 9, we show for $\varepsilon = 10^{-4}$, as time evolves, the distribution function f converges to the unified Maxwellian \bar{M} . This numerically verifies the relaxed-AP property. In Figure 10, we show evolution of u with different ε . Apparently different species gradually share the same velocity, and the smaller ε is, the faster the convergence is.

6.3 A Disparate Masses Problem

In this example, we deal with the ion-electron evolution problem. Define $\varepsilon = \sqrt{\frac{m_L}{m_H}}$, we want to verify that the light species gets close to the unified Maxwellian \bar{M}_L faster than the heavy one. We show an inhomogeneous problem with the following initial data:

$$m_H = 8, m_L = 0.08, u_H = 0.7, u_L = 0, T_H = T_L = 2.5, n_H = 1, n_L = 1.2.$$

The initial distribution f is given the same as in the previous two examples, but with C_1 and C_2 defined by: $C_1 - u = u - C_2 = \kappa$. We choose $\kappa = 0.5$. In Figure 11, we show several snapshots of the distributions of two species at different time steps. In Figure 12, we show how velocities of the two species converge toward each other.

Acknowledgements. The second author would like to thank Dr. Cory Hauck and Dr. Bokai Yan for stimulating discussions.

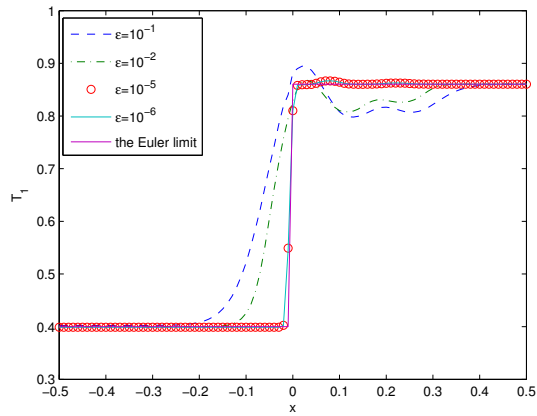
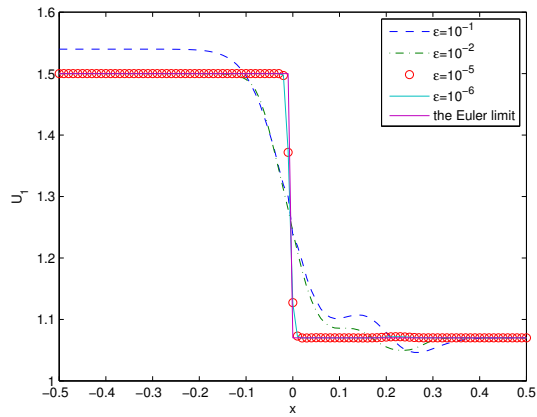
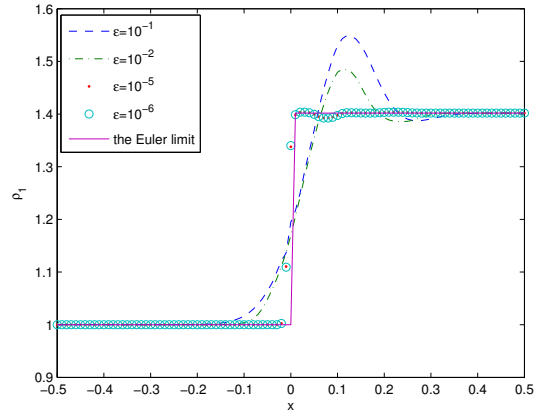


Figure 2: The Stationary Shock problem. As $\varepsilon \rightarrow 0$, solution of the Boltzmann equation goes to the Euler limit. Time $T = 0.1$.

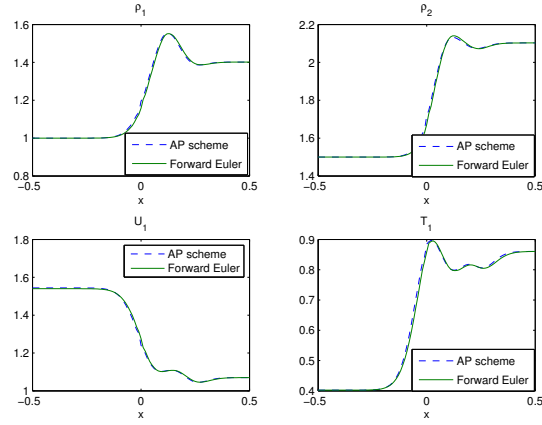


Figure 3: The Stationary Shock Problem. For $\varepsilon = 0.1$, we compare the results given by the AP scheme and the forward Euler method. They match well. Time $T = 0.1$.

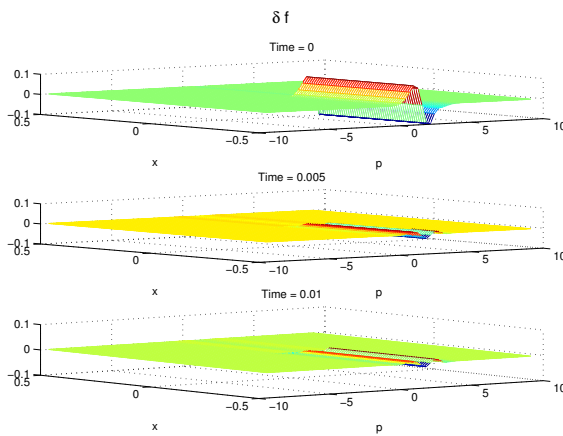


Figure 4: The Stationary Shock Problem. $\varepsilon = 10^{-5}$. As time evolves, f_1 converges to \overline{M}_1 . In the figure, $\delta f = f_1 - \overline{M}_1$.

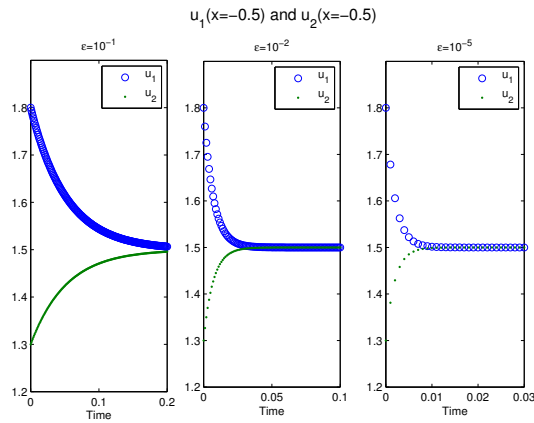


Figure 5: The Stationary Shock problem. The three figures above show velocities u_1 and u_2 at $x = -0.5$ as a function of time for $\epsilon = 10^{-1}, 10^{-2}$ and 10^{-5} respectively. The smaller ϵ is, the faster the velocities of the two species converge to each other. Noted that the time scales for three figures are different.

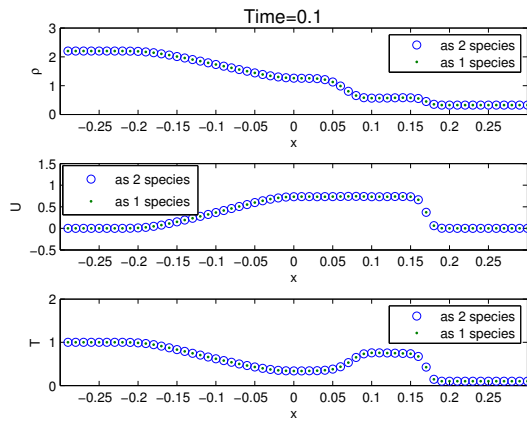
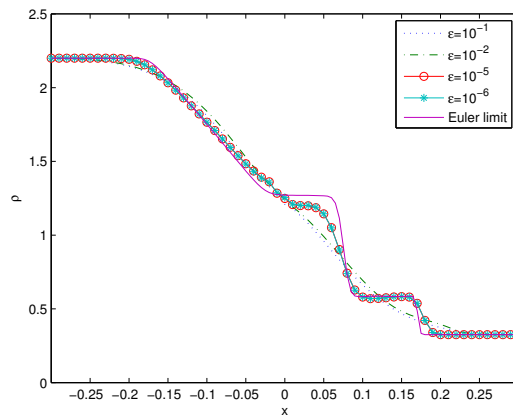


Figure 6: The Sod problem. Indifferentiability. Time $T = 0.1$.



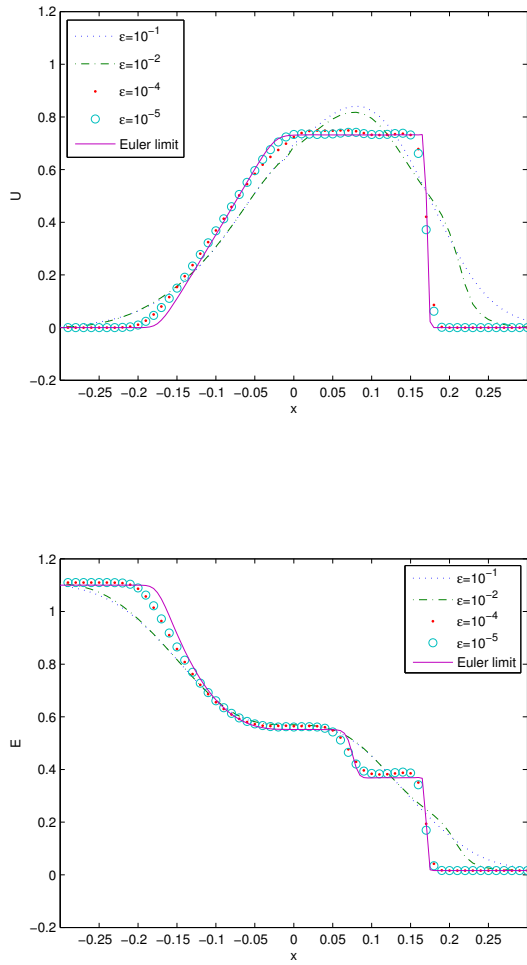


Figure 7: The Sod problem. As $\varepsilon \rightarrow 0$, the numerical results go to the Euler limit. Time $T = 0.1$.

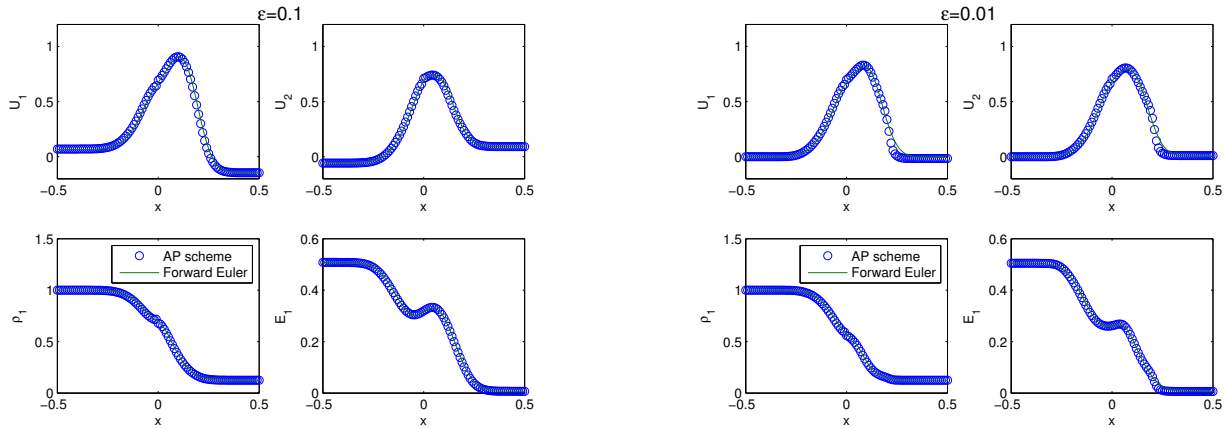


Figure 8: The Sod problem. For $\varepsilon = 0.1, 0.01$, time $T = 0.1$, we compare the results given by the new scheme and the forward Euler method. They match well.

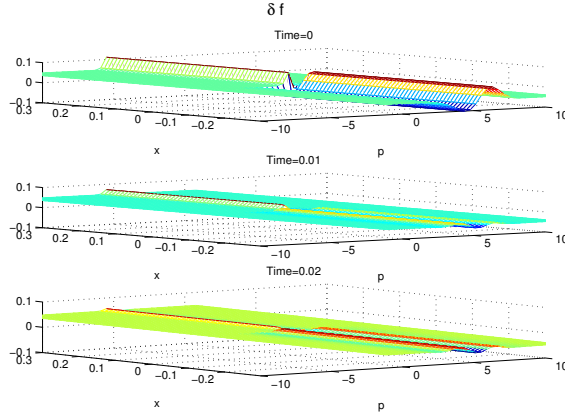


Figure 9: The Sod problem. f_1 converges to the unified Maxwellian \bar{M}_1 as t increases. Initially, f_1 is far away from \bar{M}_1 . $\varepsilon = 10^{-4}$. $\delta f = f - \bar{M}$ in the figure.

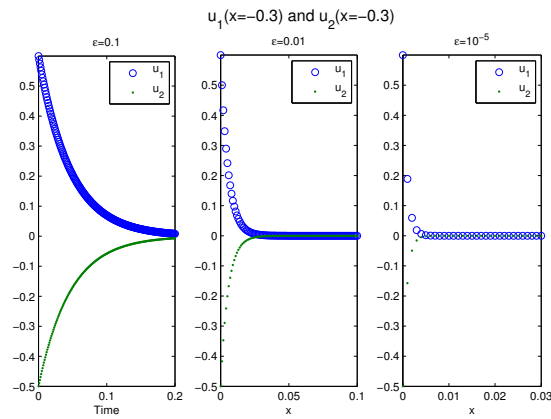


Figure 10: The Sod problem. The three figures show velocities u_1 and u_2 at $x = -0.3$ as a function of time for $\varepsilon = 0.1, 0.01$, and 10^{-5} respectively. The smaller ε is, the faster the velocities of the two species converge to each other. Noted that the ending time are different for three figures.

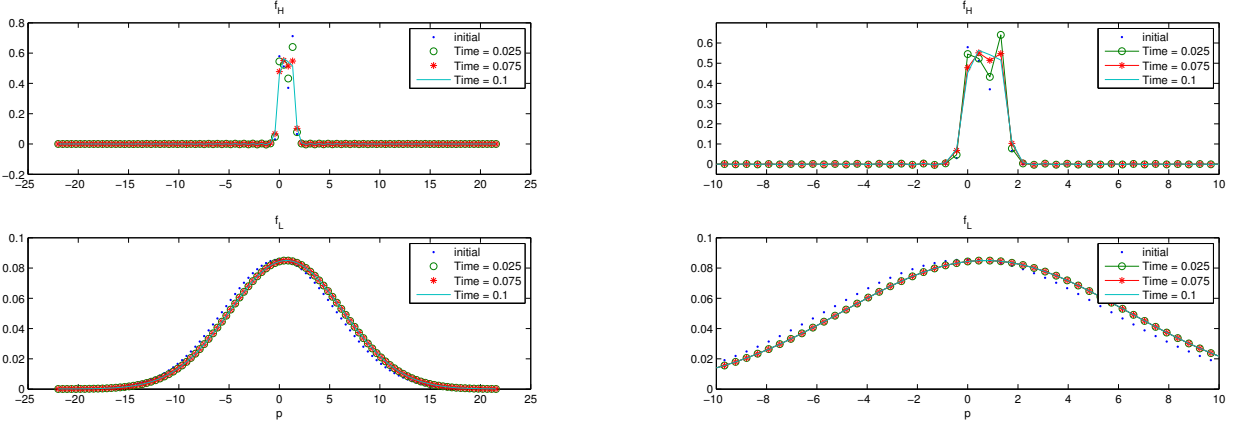


Figure 11: The disparate masses problem. Initially, both species are far away from the unified Maxwellian \bar{M} . At $T = 0.025$, the light species is already very close to \bar{M}_L while the heavy species is still far away from \bar{M}_H . At $T = 0.075$, both species are close to their final distributions. We use the distribution at $T = 0.1$ as the steady state. The figure on the right is a zoom-in.

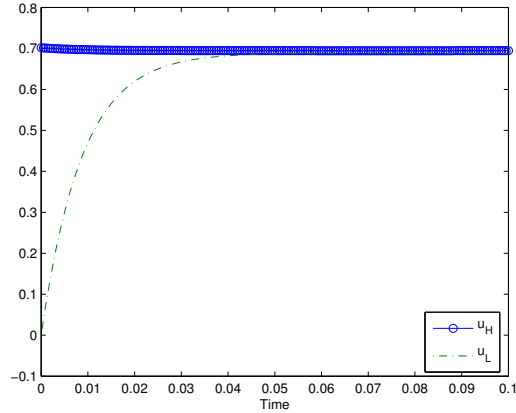


Figure 12: The disparate masses problem. The velocities for the two species converge to each other.

References

- [1] P. ANDRIES, K. AOKI, AND B. PERTHAME, *A consistent BGK-type model for gas mixtures*, Journal of Statistical Physics, 106 (2002), pp. 993–1018.
- [2] C. BESSE, S. BORGHOL, T. GOUDON, I. LACROIX-VIOLET, AND J.-P. DUDON, *Hydrodynamic regimes, Knudsen layer, numerical schemes: Definition of boundary fluxes*, Advances in Applied Mathematics and Mechanics, (to appear).
- [3] J. F. BOURGAT, P. L. TALLEC, B. PERTHAME, AND Y. QIU, *Coupling Boltzmann and Euler equations without overlapping*, in Domain Decomposition Methods in Science and Engineering, A. Quarteroni, J. Périaux, Y. A. Kuznetsov, and O. Widlund, eds., Providence, RI, 1994, AMS, pp. 377–398.
- [4] S. I. BRAGINSKII, *Transport processes in a plasma*, Reviews of Plasma Physics, 1 (1965), p. 205.
- [5] R. CAFLISCH, S. JIN AND G. RUSSO, *Uniformly Accurate Schemes for Hyperbolic Systems with Relaxations*, SIAM J. Numerical Analysis 34, 246-281 (1997).
- [6] R. M. CHMIELESKI AND J. H. FERZIGER, *Transport properties of a nonequilibrium partially ionized gas*, Physics of Fluids, 10 (1967), pp. 364–371.
- [7] F. CORON AND B. PERTHAME, *Numerical passage from kinetic to fluid equations*, SIAM J. Numer. Anal. 28 (1991) pp. 26-42.
- [8] P. DEGOND AND S. JIN, *A smooth transition model between kinetic and diffusion equations*, SIAM J. Numer. Anal., 42 (2005), pp. 2671–2687.
- [9] P. DEGOND, S. JIN, AND L. MIEUSSENS, *A smooth transition model between kinetic and hydrodynamic equations*, J. of Comput. Phys., 209 (2005), pp. 665 – 694.
- [10] P. DEGOND AND B. LUCQUIN-DESREUX, *The asymptotics of collision operators for two species of particles of disparate masses*, Mathematical Models and Methods in Applied Sciences, 6 (1996), pp. 405–436.
- [11] ———, *Transport coefficients of plasmas and disparate mass binary gases*, Transport Theory and Statistical Physics, 25 (1996), pp. 595–633.
- [12] G. DIMARCO AND L. PARESCHI, *Exponential Runge-Kutta methods for stiff kinetic equations*, arXiv:1010.1472, (October 2010).
- [13] J. H. FERZIGER AND H. G. KAPER, *Mathematical Theory of Transport Processes in Gases*, North-Holland Pub. Co, 1972.
- [14] F. FILBET, J.W. HU AND S. JIN, *A numerical scheme for the quantum Boltzmann equation with stiff collision terms*, Math. Model Num. Anal., to appear.
- [15] F. FILBET AND S. JIN, *A class of asymptotic-preserving schemes for kinetic equations and related problems with stiff sources*, J. Comput. Phys., 229 (2010), pp. 7625–7648.
- [16] F. FILBET AND A. RAMBAUD, *Analysis of an asymptotic preserving scheme for relaxation systems*, arXiv:1105.2655v1.
- [17] E. GABETTA, L. PARESCHI, AND G. TOSCANI, *Relaxation schemes for nonlinear kinetic equations*, SIAM J. Numer. Anal, 34 (1997), pp. 2168–2194.

- [18] V. GARZÒ, A. SANTOS, AND J. J. BREY, *A kinetic model for a multicomponent gas*, Physics of Fluids, 1 (1989), pp. 380–384.
- [19] E. GOLDMAN AND L. SIROVICH, *Equations for gas mixtures*, Physics of Fluids, 10 (1967), pp. 1928–1940.
- [20] F. GOLSE, S. JIN, AND C. D. LEVERMORE, *A domain decomposition analysis for a two-scale linear transport problem*, Math. Model Num. Anal, 37 (2002), pp. 869–892.
- [21] H. GRAD, in *Rarefied Gas Dynamics*, F. Devienne, ed., Pergamon, London, England, 1960, pp. 10–138.
- [22] E. P. GROSS AND M. KROOK, *Model for collision processes in gases: Small-amplitude oscillations of charged two-component systems*, Phys. Rev., 102 (1956), pp. 593–604.
- [23] M. GUENTHER, J. STRUCKMEIER, P. L. TALLEC, AND J. PERLAT, *Numerical modeling of gas flows in the transition between rarefied and continuum regimes*, Notes on Numerical Fluid Mechanics, 66 (1998), pp. 222–241.
- [24] J.W. HU, S. JIN AND B.K. YAN, *A numerical scheme for the quantum Fokker-Planck-Landau equation efficient in the fluid regime*, Commun. Comp. Phys., submitted.
- [25] S. JIN, *Runge-Kutta Methods for Hyperbolic Conservation Laws with Stiff Relaxation Terms*, J. Computational Physics, 122 (1995), 51-67.
- [26] S. JIN, *Efficient asymptotic-preserving (AP) schemes for some multiscale kinetic equations*, SIAM J. Sci. Comp, 21 (1999), pp. 441–454.
- [27] S. JIN, *Asymptotic preserving (AP) schemes for multiscale kinetic and hyperbolic equations: a review*, Lecture Notes for Summer School on "Methods and Models of Kinetic Theory" (M&MKT), Porto Ercole (Grosseto, Italy), June 2010. Rivista di Matematica della Universita di Parma, to appear
- [28] S. JIN AND Y. SHI, *A micro-macro decomposition-based asymptotic-preserving scheme for the multispecies Boltzmann equation*, SIAM J. Sci. Comput., 31 (2010), pp. 4580–4606.
- [29] S. JIN AND B.K. YAN, *A class of asymptotic-preserving schemes for the Fokker-Planck-Landau equation*, J. Comp. Phys. 230(2011), 6420-6437.
- [30] S. JIN, X. YANG, AND G. YUAN, *A domain decomposition method for a two-scale transport equation with energy flux conserved at the interface, kinetic and related models*, Kinetic and Related Models, 1 (2008), pp. 65–84.
- [31] E. A. JOHNSON, *Energy and momentum equations for dispartemass binary gases*, Physics of Fluids, 16 (1973), pp. 45–49.
- [32] A. KLAR, H. NEUNZERT, AND J. STRUCKMEIER, *Transition from kinetic theory to macroscopic fluid equations: A problem for domain decomposition and a source for new algorithms*, Transport Theory and Statistical Physics, 29 (2000), pp. 93–106.
- [33] M. LEMOU AND L. MIEUSSENS, *A new asymptotic preserving scheme based on micro-macro formulation for linear kinetic equations in the diffusion limit*. SIAM J. Sci. Comput. 31 (2008) no. 1, 334-368.

- [34] R. J. LEVEQUE, *Numerical Methods for Conservation Laws*, Lectures in mathematics ETH Zürich, Birkhäuser Verlag, 1992.
- [35] R. J. LEVEQUE AND ETC., Version 4.3. "<http://www.amath.washington.edu/claw/>".
- [36] L. PARESCHI AND G. RUSSO, *Numerical solution of the Boltzmann equation I: Spectrally accurate approximation of the collision operator*, SIAM J. Numer. Anal, 37 (2000), pp. 1217–1245.
- [37] L. SIROVICH, *Kinetic modeling of gas mixtures*, Physics of Fluids, 5 (1962), pp. 908–918.
- [38] L. SPITZER AND R. HÄRM, *Transport phenomena in a completely ionized gas*, Phys. Rev., 89 (1953), pp. 977–981.
- [39] P. L. TALLEC AND F. MALLINGER, *Coupling Boltzmann and Navier-Stokes equations by half fluxes*, J. Comput. Phys., 136 (1997), pp. 51 – 67.
- [40] A. F. VASSEUR, *Rigorous derivation of the kinetic/fluid coupling involving a kinetic layer on a toy problem*, Archive for Rational Mechanics and Analysis, (to appear).